Formability of Al–Nb Bearing Ultra High-strength TRIP-aided Sheet Steels with Bainitic Ferrite and/or Martensite Matrix

Koh-ichi SUGIMOTO,[1] Muneo MURATA[2] and Sung-Moo SONG[1]

1) Faculty of Engineering, Shinshu University, 4-17-1 Wakasato, Nagano 380-8553 Japan.
2) Formerly Graduate Student, Graduate School of Science and Technology, Shinshu University, 4-17-1 Wakasato, Nagano 380-8553 Japan. Now at Toyota Motor Co.

Microstructure, tensile properties and stretch-flangeability of 980–1 470 MPa grade Al or Al–Nb bearing TRIP-aided cold-rolled sheet steels with bainitic ferrite and/or martensite matrix microstructure (TBF steels) were investigated for automotive applications such as impact member reinforcements, sheet flames and so on. In addition, these properties were related with the microstructure and the retained austenite characteristics. Complex additions of 0.5 % Al and 0.05 % Nb into a base steel with chemical composition of 0.2 % C, 1.5 % Si and 1.5 % Mn (in mass%) significantly enhanced the total elongation and stretch-flangeability, especially when austempered at temperatures below martensite-start temperature. The excellent stretch-flangeability was primarily associated with (i) refined prior austenitic grain by NbC precipitates and (ii) uniform fine mixed matrix microstructure of bainitic ferrite and martensite, as well as (iii) TRIP effect of metastable retained austenite.

KEY WORDS: strech-flangeability; ultra high-strength steel; TRIP-aided steel; retained austenite; martensite; bainitic ferrite; microalloying.

1. Introduction

In order to attain a drastic weight reduction and crash worthiness performance, automotive members such as a center-pillar *etc.* with tensile strength of 980–1 470 MPa are fabricated by hot press process (hot-forming or die quenching)[1,2] because of difficulty of cold stamping. However, the hot press process is characterized by a poor cost performance for production, so that formable ultra high-strength steels for cold stamping are required for the press members.

In low alloy TRIP-aided steels, the transformation-induced plasticity (TRIP)[3] of retained austenite is very useful in improving the room temperature formability of high-strength steels. On the basis of such a fact, 780–1 470 MPa grade C–Si–Mn TRIP-aided steels with bainitic ferrite matrix or TRIP-aided bainitic ferrite steels (TBF steels) were recently developed by our research group.[4–9]

According to a previous research,[6–9] alloying elements like C, Si, Mn, Nb, Mo *etc.* control the formability of the TBF steel. However, any effects of Al and/or Nb on the formability are not examined yet. In this study, the effects of Al addition and Al–Nb complex addition on the tensile property and formability of 0.2%C–1.5%Si–1.5%Mn TBF steels were investigated. In addition, these results were related with metallurgical factors such as microstructure and retained austenite characteristics.

2. Experimental Procedure

In this study, three kinds of steels with different Si, Al and Nb contents were prepared as vacuum-melted 100 kg ingots, followed by hot forging to produce 30 mm thick slabs. Chemical composition of these slabs is shown in **Table 1**, in which martensite start temperature (M_s) was calculated using the empirical relation[10] and total content of Si and Al was fixed to be constant (1.5 mass%).

The slabs were reheated to 1 200°C and were hot-rolled to a thickness of 3.2 mm, finishing at 850°C and then coiled at 600°C, as shown in **Fig. 1**. After cold rolling to a thickness of 1.2 mm, the sheets were annealed at 950°C and then austempered at 300–500°C for 200 s in salt bath.

The volume fraction of retained austenite was quantified from integrated intensity of $(200)\alpha$, $(211)\alpha$, $(200)\gamma$, $(220)\gamma$ and $(311)\gamma$ peaks of Mo-Kα radiation.[11] The carbon concentration (C_γ, mass%) was estimated by substituting the lattice constant (a_γ, 10^{-10} m) measured from $(220)\gamma$ peak of Cu-Kα radiation into the following equation proposed by Dyson and Holmes,[12]
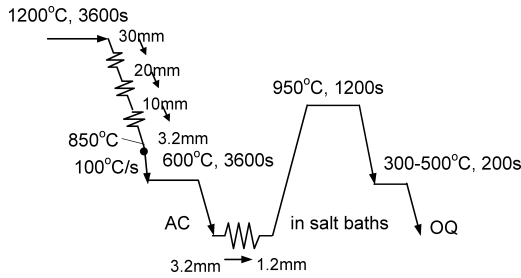
Table 1. Chemical composition and estimated martensite-start temperature (M_s) of steels used.

steel	C	Si	Mn	P	S	Al	Nb	N	M_s
				(mass%)					(°C)
A	0.19	1.54	1.51	0.006	0.0025	0.038	—	0.0022	423
B	0.20	0.99	1.51	0.005	0.0026	0.490	—	0.0017	433
C	0.20	1.00	1.50	0.015	0.0025	0.480	0.049	0.0009	433

$$a_\gamma = 3.5780 + 0.0330 \times (\%C_\gamma) + 0.00095 \times (\%Mn_\gamma) - 0.0002$$
$$\times (\%Ni_\gamma) + 0.0006 \times (\%Cr_\gamma) + 0.0056 \times (\%N_\gamma) + 0.0028$$
$$\times (\%Al_\gamma) - 0.0004 \times (\%Co_\gamma) + 0.0014 \times (\%Cu_\gamma)$$
$$+ 0.0053 \times (\%Mo_\gamma) + 0.0079 \times (\%Nb_\gamma) + 0.0032$$
$$\times (\%Ti_\gamma) + 0.0017 \times (\%V_\gamma) + 0.0057 \times (\%W_\gamma) \quad \ldots\ldots\ldots(1)$$

where $\%Mn_\gamma$, $\%Ni_\gamma$, $\%Cr_\gamma$, $\%N_\gamma$, $\%Al_\gamma$, $\%Co_\gamma$, $\%Cu_\gamma$, $\%Mo_\gamma$, $\%Nb_\gamma$, $\%Ti_\gamma$, $\%V_\gamma$ and $\%W_\gamma$ represent solute content (mass%) of the individual alloying elements in retained austenite. For convenience, they were assumed to be equivalent to added contents.

Tensile tests were carried out on a hard type of testing machine using specimens with gage length of 50 mm, gage width of 12.5 mm and thickness of 1.2 mm. The hole-expanding ratio (λ) was determined by the following equation.

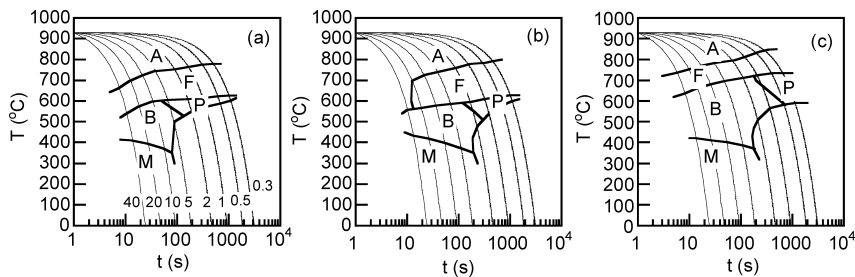$$\lambda = \{(d_f - d_0)/d_0\} \times 100\% \ldots\ldots\ldots\ldots(2)$$

where d_0 and d_f are initial hole diameter (4.76 mm) and hole diameter on cracking, respectively. Cross head speeds on hole-punching and hole-expanding are 10 mm/min and 1 mm/min, respectively. The clearance between die and punch was 10% of sheet thickness. All the tests were conducted at 25°C.

3. Results

3.1. Microstructure and Retained Austenite Characteristics

Figure 2 shows CCT curves of steels A, B and C which are measured using Formaster. From these figures, it is found that Al in solid solution suppresses ferrite transformation. On the other hand, Nb in solid solution promotes the transformation, differing from the result of DeArdo *et al.*[13] In addition, the Nb extends bainite transformation temperature range.

Figure 3 shows typical micrographs of steels A, B and C

Fig. 1. Schematic diagram of hot and cold rolling processes and annealing and then austempering process of TBF steels, in which "AC" and "OQ" represent air cooling and quenching in oil, respectively.

Fig. 2. Continuous cooling transformation diagrams of steels (a) A, (b) B and (c) C, in which "A", "F", "P", "B" and "M" represent austenite, ferrite, pearlite, bainite and martensite, respectively. Numerals in (a) denote cooling rate (°C/s).
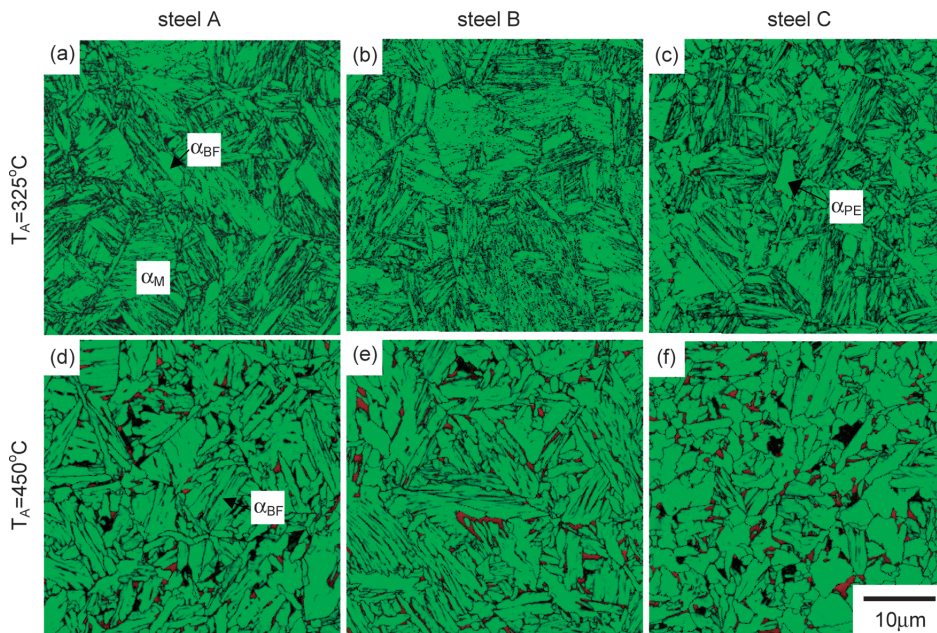
Fig. 3. Typical microstructure of steels A–C austempered at 325°C or 450°C, in which α_M, α_{BF} and α_{PE} are martensite, bainitic ferrite and pro-eutectoid ferrite, respectively. Green: matrix, red: retained austenite.
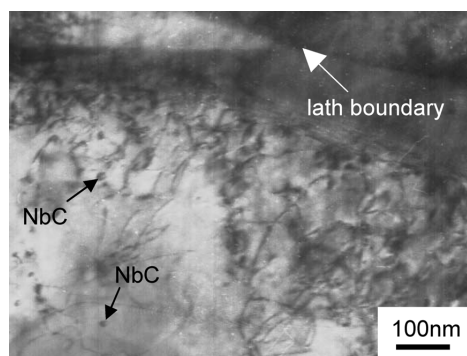
Fig. 4. Transmission electron micrographs of matrix in steel C austempered at 450°C.

austempered at 325°C or 450°C, respectively. When austempered at temperatures below M_s, microstructure of steel A consists of martensite/bainitic ferrite mixed matrix and interlath retained austenite. The martensite fraction tends to increase with decreasing austempering temperature. On the other hand, when austempered at temperatures above M_s, the matrix microstructure changes into bainitic ferrite.

In steel C, however, a small amount of pro-eutectoid ferrite is nucleated and prior austenite grain is refined when austempered at temperatures below M_s. If austempered at temperatures above M_s, the matrix microstructure changes into granular bainitic ferrite and resultantly the retained austenite phase changes to be blocky. In this case, a large amount of NbC precipitates of about 10–50 nm in diameter are observed in the matrix (**Fig. 4**). As mentioned later, the NbC precipitates contribute to grain refining of prior austenite, not precipitation hardening of matrix.

Steel B was characterized by the same microstructure as steel A, although lath size of the matrix was refined, compared with steel A.

Figure 5 shows the variations of initial retained austenite characteristics as a function of austempering temperature of steels A, B and C. Al addition considerably increases the carbon concentration of retained austenite ($C_{\gamma 0}$) although it decreases its volume fraction ($f_{\gamma 0}$). In addition, it raises austempering temperature for peak total carbon concentration of retained austenite ($f_{\gamma 0} \times C_{\gamma 0}$) up to 450°C. Further addition of Nb decreases the carbon concentration of retained austenite, but its volume fraction is increased. Note that optimum austempering temperature (450°C) for the volume fraction of retained austenite in steels B and C is nearly equal to the hot-dip galvanizing temperature (about 460°C).

3.2. Tensile Properties

Figure 6 shows stress–strain curves of steel B. **Figure 7** shows the variations in yield stress (0.2% offset proof stress; *YS*), tensile strength (*TS*) and yield ratio (*YR*) with austempering temperature in steels A, B and C. Al addition decreases the yield stress and tensile strength due to removal of the same amount of Si. On the other hand, further addition of Nb hardly increases these strengths, despite the existence of fine NbC precipitates. Yield ratios of the steels B and C are nearly the same as steel A when austempered at 350–425°C, but these steels possess higher yield ratios
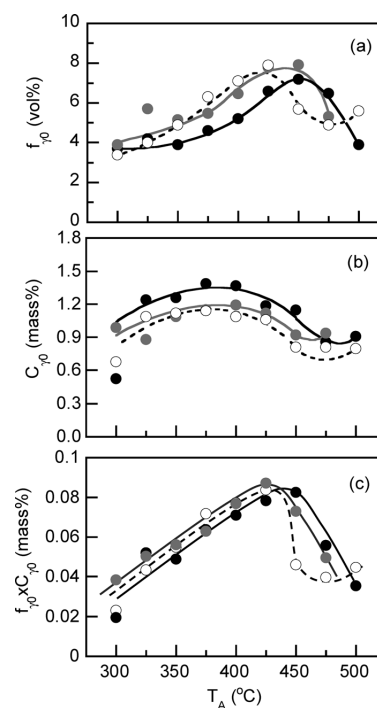

Fig. 5. Variations in (a) initial volume fraction ($f_{\gamma 0}$), (b) initial carbon concentration ($C_{\gamma 0}$) and (c) initial total carbon concentration ($f_{\gamma 0} \times C_{\gamma 0}$) of retained austenite as a function of austempering temperature (T_A) in steels A (○), B (●) and C (●).
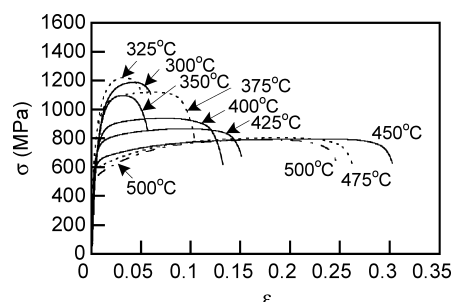

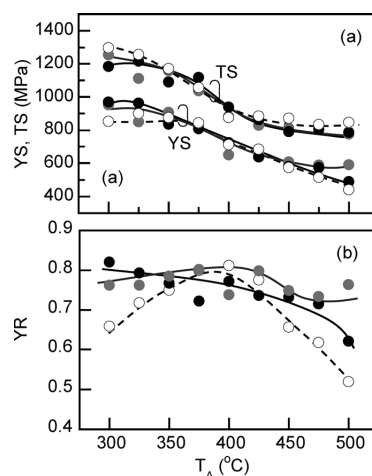**Fig. 6.** Changes in engineering flow curves of steel B austempered at 300–500°C.

Fig. 7. Variations in (a) yield stress (*YS*), tensile strength (*TS*) and (b) yield ratio (*YR*=*YS/TS*) as a function of austempering temeperature (T_A) of steels A (○), B (●) and C (●).
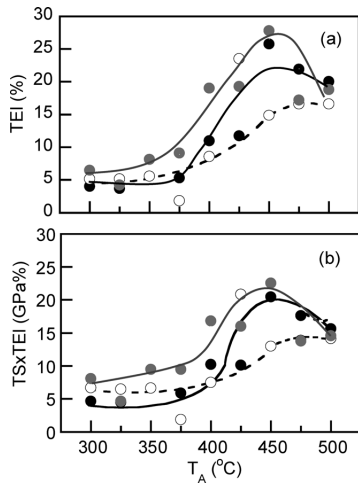
than steel A when austempered at other temperatures. The higher yield ratios are owing to an appearance of yield point (see Fig. 6).

Figure 8 shows austempering temperature dependences of total elongation (*TEl*) and combination of tensile strength and total elongation (*TS*×*TEl*) of the steels A, B and C. The total elongation and the combination of tensile strength and total elongation are increased by complex addition of Nb and Al. Al addition is effective on improvement of the total elongation and the combination, only when austempered at temperatures above 400°C.

3.3. Stretch-flangeability

Figure 9 shows hole-expanding ratio (λ) and combination of tensile strength and stretch-flangeability (*TS*×λ) in the steels A, B and C. Excellent stretch-flangeability is achieved in the steel C austempered below M$_s$. Note that such a good stretch-flangeability above 50 GPa% has been not reported up to now.

Figure 10 shows the variations in a length of shear section (*ss*) on hole-punching as a function of austempering temperature in steels A, B and C. It is found that the shear section length is increased in steels B and C. It is noteworthy that the void and/or crack initiation and growth at break section are suppressed in the steel C, as shown in Fig. 11.

4. Discussion

4.1. Microstructural Change during Austempering

When steels A, B and C were austempered at temperatures lower than M$_s$, these matrix microstructures were composed of martensite and bainitic ferrite, similar to the steel subjected to quenching–partitioning (Q&P) process.[14] From Figs. 2 and 3, such a mixed matrix microstructure may be formed as follows.

(1) In these steels, a small amount of pro-eutectoid ferrite (α_{PE}) and bainitic ferrite (α_{BF}) first initiate during cooling after annealing in γ region (stage 2 of Figs. 12(a), 12(c)) because the hardenability is relatively low.

(2) On continuous cooling to temperatures below M$_s$,
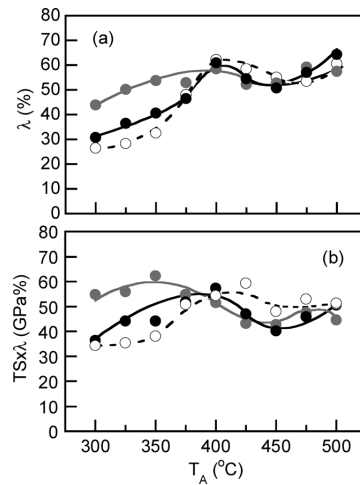
Fig. 9. Variations in (a) hole-expanding ratio (λ) and (b) strength stretch-flangeability balance (*TS*×λ) as a function of austempering temperature (*T*$_A$) in steels A (○), B (●) and C (◐).

Fig. 8. Variations in (a) total elongation (*TEl*) and (b) strength–ductility balance (*TS*×*TEl*) as a function of austempering temperature (*T*$_A$) in steels A (○), B (●) and C (◐).
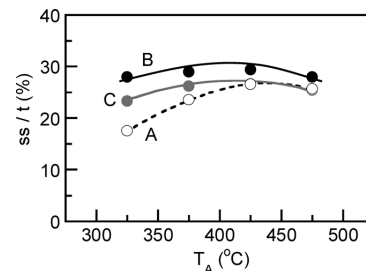
Fig. 10. Ratio (*ss*/*t*) of shear section length to sheet thickness as a function of austempering temperature (*T*$_A$) in steels A (○), B (●) and C (◐).
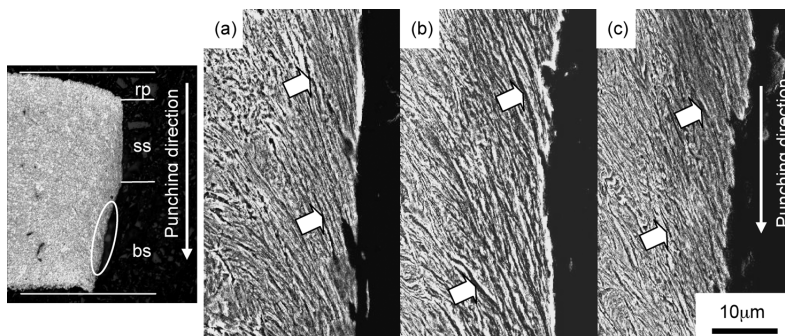
Fig. 11. SEM images of break section of (a) steels A, (b) B and (c) C austempered at 325°C, in which arrows represent narrow cracks initiated on hole-punching. rp: roll-over portion, ss: shearing section, bs: break section.

© 2010 ISIJ
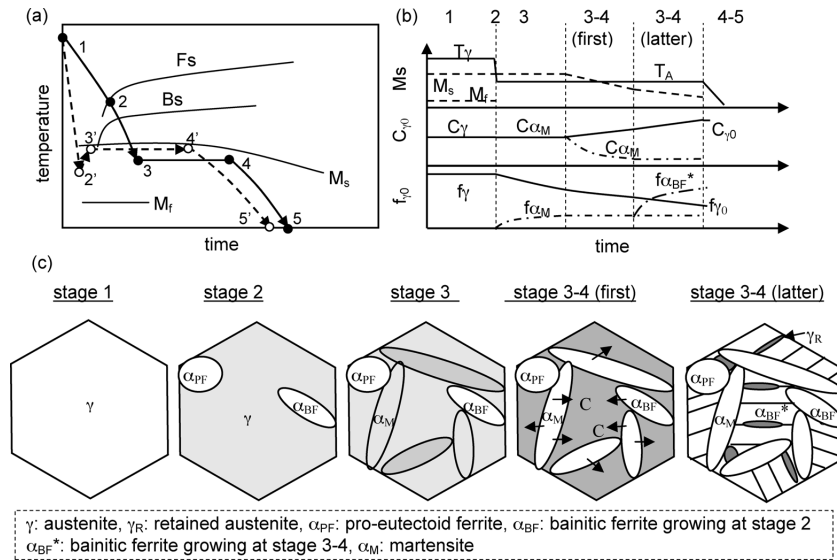
Fig. 12. Illustrations of (a) heat treatment diagram for TBF (solid line) and Q&P steels (dotted line, two step Q&P process), (b) variations in M_s temperature of austenite, carbon concentration of austenite and martensite ($C\gamma$, $C\alpha_M$) and volume fraction of each phase ($f\gamma$, $f\alpha_M$, $f\alpha_{BF}*$) and (c) microstructural change[15] at stages 1 through 5.

some of austenite transforms to martensite (α_M) (stage 3 in Figs. 12(a), 12(c)). The amount of martensite tends to increase with decreasing austempering temperature in a temperature range between M_s and M_f.

(3) In stage 3–4, most of solute carbon in the transformed martensite first diffuses to austenite. As carbon-enrichment in austenite proceeds, M_s temperature of austenite lowers up to temperature lower than austempering temperature (see M_s in Fig. 12(b)). Consequently the austenite starts to transform to bainitic ferrite ($\alpha_{BF}*$), differing from initial bainitic ferrite (α_{BF}) of the above (1).

(4) By cooling after austempering (stage 4–5), untransformed austenite is retained.

The above process differs somewhat from two step Q&P process (dotted line in Fig. 12(a)) proposed by Speer *et al.*[14] However, it agrees well with one step Q&P process,[14] except for a small amount of pro-eutectoid ferrite and bainitic ferrite transformed at stage 2.

Kim *et al.*[15] reported that a difference in temperature between M_s and M_f of steel with resemble chemical composition with the present steel is about 133°C. This indicates that M_f temperatures of the present steels are about 290–300°C lower than austempering temperatures of this study. So, volume fraction of martensite in martensite/bainitic ferrite mixed matrix can be estimated by Koistinen–Marburger model[16] in steels austempered at temperatures between 400°C and 300°C.

4.2. Roles of Al and Nb on Microstructure and Retained Austenite Characters

In Fig. 5(b), steel B possessed high carbon concentration of retained austenite, with a decrease in its volume fraction. According to a previous study on low alloyed TRIP-aided steels with polygonal ferrite matrix (TPF steel)[17–19] and with annealed martensite matrix (TAM steel),[17] Al addition of 0.5–1.0 mass% increases the carbon concentration of retained austenite because Al raises T_0 temperature at which austenite and ferrite of the same chemical composition have identical free energies.[20] So, high carbon concentration of

steel B is considered to be owing to the increased T_0 temperature.

In Fig. 3, microstructure of steel C was refined so much. Also, the steel contained a small amount of pro-eutectoid ferrite. The former may be caused by NbC precipitates of 10–50 nm (Fig. 4), which contributes to suppress the grain growth.[8] The latter is associated with a lack of hardenability as shown in Fig. 2(c). According to DeArdo *et al.*,[13] Nb in solid solution suppresses ferrite transformation, similar to Al. So, it is considered that grain refining (an increase in grain boundary area) due to NbC deteriorated the hardenability in the steel C.

Carbon concentration of retained austenite was decreased by Nb addition, with the increased volume fraction of retained austenite (Fig. 5). The same result has been also reported by Sugimoto *et al.*[8] Since Nb is not influence T_0 temperature, carbon consumption by NbC precipitates may be associated with the decreased carbon concentration of retained austenite.

4.3. Excellent Total Elongation

In the conventional TRIP-aided steels, microalloying by Nb of 0.02–0.05 mass% improves the strength–elongation balance.[21–25] In this case, the increased strength–elongation balance is caused by refining of matrix microstructure and retained austenite phase due to NbC precipitates. Also, the strength–elongation balance is controlled by volume fraction and stability (carbon concentration) of retained austenite, as well as retained austenite morphology, according to Sugimoto *et al.*[5,19,26–28]

In the present study, Nb addition into the steel B brought on an excellent strength–elongation balance, even when austempered at much lower temperatures than M_s. As shown in **Fig. 13**(a), the strength–elongation balance of steel C showed a positive relationship with the volume fraction of retained austenite, in the same way as steels A and B. Also, it has a positive correlation with carbon concentration of retained austenite although the correlation is divided into two retained austenite fraction regions of 3–5 vol%
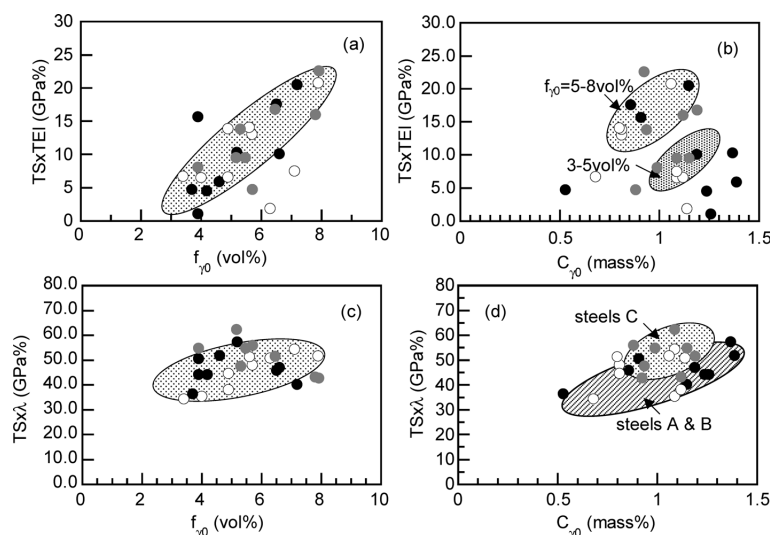
Fig. 13. Correlations between (a, b) strength–elongation balance ($TS \times TEl$) and (c, d) strength-stretch-flangeability balance ($TS \times \lambda$) and initial volume fraction ($f_{\gamma 0}$) and initial carbon concentration ($C_{\gamma 0}$) of retained austenite of steels A (○), B (●) and C (●).

(T_A=300–375°C) and 5–8 vol% (T_A=400–75°C), as shown in Fig. 13(b). From these facts, it is found that the excellent strength–elongation balance of the steel C austempered at temperatures above M_s is caused by TRIP effect of a large amount of metastable retained austenite. In this case, the matrix microstructure was characterized by fine granular microstructure (Fig. 3(f)). Therefore, a high long range internal stress[28] resulting from soft granular matrix microstructure and hard blocky retained austenite phase may contribute to the excellent strength–elongation balance, as well as suppression of void initiation due to uniformly refined microstructure.

When the steel C was austempered at temperatures below M_s, relatively large total elongation was completed. The reason is in consideration.

4.4. Excellent Stretch-flangeability

Sugimoto *et al.*[5,6] have reported that the stretch-flangeability of TBF steel is controlled by (i) volume fraction and stability of retained austenite and uniformity and (ii) size of matrix microstructure which influence both the hole-surface layer damage on punching and the localized ductility on expanding.

The present steel C exhibited an excellent stretch-flangeability, when austempered at low temperatures below M_s (Fig. 9), despite high tensile strength above 1 100 MPa. From the following facts, it is considered that the superior stretch-flangeability of steel C is primarily caused by uniform refined matrix and retained austenite, resulting in small punching damage. Also, the metastable retained austenite may contribute to high localized ductility through significant TRIP effect on expanding.

(1) The strength-stretch-flangeability balance of the steel C was linearly correlated with carbon concentration of retained austenite (Fig. 13(d)).

(2) Although the steel C contained a small amount of pro-eutectoid ferrite in matrix (Fig. 3(c)), the prior austenite grain size was considerably refined due to NbC precipitaes.

(3) Resultantly, the steel C exhibited relatively long shear

section on hole punching (Fig. 10). In addition, only small and narrow cracks were formed at the break section of the steel C (Fig. 11).

5. Conclusions

The effects of additions of Al or Al–Nb on the microstructure, tensile properties and stretch-flangeability of 0.2%C–1.5%Si–1.5%Mn TBF steels were investigated. Main results were summarized as follows,

(1) Al played a role of stabilizing mechanically retained austenite through increasing the carbon concentration. On the other hand, further addition of Nb refined the structures of matrix and retained austenite due to NbC precipitates, although it changed the morphology of both the phases and lowered the mechanical stability of retained austenite. In addition, Nb addition promoted a nucleation of pro-eutectoid ferrite.

(2) Complex addition of Al and Nb increased total elongation of the TBF steel, especially in a tensile strength range above 1 000 MPa. Also, it improved considerably the stretch-flangeability. The increased stretch-flangeability was primarily associated with (i) refined prior austenitic grain by NbC precipitates and (ii) uniform fine mixed matrix microstructure of bainitic ferrite and martensite, as well as (iii) TRIP effect of metastable retained austenite.

REFERENCES

1) M. Suehiro, K. Kusumi, T. Miyakoshi, J. Maki and M. Ohgami: *Nippon Steel Tech. Rep.*, No. 88, (2003), 16.
2) A. Turetta, S. Bruschi and A. Ghioti: *J. Mater. Process. Technol.*, **177**

(2006), 396.

3) V. F. Zackay, E. R. Parker, D. Fahr and R. Busch: *Trans. Am. Soc. Met.*, **60** (1967), 252.

4) K. Sugimoto, T. Iida, J. Sakaguchi and T. Kashima: *ISIJ Int.*, **40** (2000), 902.

5) K. Sugimoto, J. Sakaguchi, T. Iida and T. Kashima: *ISIJ Int.*, **40**, (2000), 920.

6) K. Sugimoto, K. Nakano, S. Song and Kashima: *ISIJ Int.*, **42**, (2002), 450.

7) K. Sugimoto, M. Tsunezawa, T. Hojo and S. Ikeda: *ISIJ Int.*, **44** (2004), 1608.

8) K. Sugimoto, M. Murata, T. Muramatsu and Y. Mukai: *ISIJ Int.*, **47** (2007), 1357.

9) K. Sugimoto, S. Hashimoto and Y. Mukai: *J. Mater. Process. Technol.*, **177/1–3** (2006), 390.

10) I. Tamura: Strength of Steels, Nikkan-Kogyo Shinbun, Tokyo, (1970), 40.

11) H. Maruyama: *J. Jpn. Soc. Heat Treat.*, **17** (1977), 198.

12) D. J. Dyson and B. Holmes: *J. Iron Steel Inst.*, **208** (1970), 469.

13) A. J. DeArdo: *Int. Met. Rev.*, **48** (2003), 371.

14) J. G. Speer, D. V. Edmonds, F. C. Rizzo and D. K. Matlock: *Solid State Mater. Sci.*, **8** (2004), 219.

15) S. J. Kim, J. G. Speer, H. S. Kim and B. C. De Cooman: Proc. of Int. Conf. on New Developments in Advanced High-Strength Sheet Steel, AIST, Warrendale, PA, (2008), 179.

16) D. P. Koistinen and R. E. Marburger: *Acta Metall.*, **7** (1959), 59.

17) N. Imai, N. Komatsubara and K. Kunishige: *CAMP-ISIJ*, **8** (1995), 572.

18) B. C. Decooman: *Solid State Mater. Sci.*, **8** (2004), 285.

19) K. Sugimoto, B. Yu, Y. Mukai and S. Ikeda: *ISIJ Int.*, **45** (2005), 1194.

20) M. Takahashi, and H. K. D. H. Bhadeshia: *Mater. Trans. JIM*, **32** (1991), 689.

21) W. Bleck, A. Frehn and J. Ohlert: Proc. Int. Symp. Niobium 2001, TMS, Warrendale, PA, (2001), 727.

22) K. Hulka, W. Bleck and K. Papamantellos: 41st MWSP Conf. Proc., ISS, Warrendale, PA, (1999), 67.

23) T. Heller and A. Nuss: Proc. of Int. Symp. on Transformation and Deformation Mechanism in Advanced High-strength Steels, Met. Soc., (2003), 7.

24) D. Krizan and B. C. Decooman: Int. Conf. on Advanced High Strength Sheet Steels for Automotive Applications Proc., AIST, Warrendale, PA, (2004), 205.

25) A. Z. Hanzaki, P. D. Hodgson and S. Yue: *ISIJ Int.*, **35** (1995), 79.

26) K. Sugimoto, N. Usui, M. Kobayashi and S. Hashimoto: *ISIJ Int.*, **32** (1992), 1311.

27) K. Sugimoto, M. Misu, M. Kobayash and H. Shirasawa: *ISIJ Int.*, **33** (1993), 775.

28) K. Sugimoto, M. Kobayashi, H. Matsushima and S. Hashimoto: *Trans. Jpn. Soc. Mech. Eng.*, **61A** (1995), 80.